# Thermal Performance of EV and HEV Battery Modules and Packs

Ahmad A. Pesaran, Ph.D., Andreas Vlahinos, Ph.D. and Steven D. Burch
Center for Transportation Technologies and Systems
National Renewable Energy Laboratory
1617 Cole Boulevard
Golden, Colorado 80401
E-mail: ahmad_pesaran@nrel.gov

## Abstract

Thermal issues associated with electric vehicle (EV) and hybrid electric vehicle (HEV) battery packs can significantly affect performance and life cycle. Temperature variations from module to module in a battery pack could result in reduced performance. As part of the U.S. Department of Energy's Hybrid Propulsion Systems Program, the National Renewable Energy Laboratory (NREL) works with automobile and battery manufacturers on thermal analysis and management of valve-regulated lead-acid battery packs for HEVs. We use fundamental heat transfer principles and finite element analysis tools to predict the temperature distributions in cells, modules, and packs. We use infrared photography and liquid crystal thermography to obtain thermal images of the surface of battery modules under HEV charge/discharge profiles. In this paper, we provide an overview of related literature on battery thermal management, along with non-proprietary results of some of our work.

## Introduction

The performance and life-cycle costs of electric vehicles (EV) and hybrid electric vehicles (HEV) depend inherently on energy storage systems such as batteries. Battery pack performance directly affects the all-electric (zero-emission) range, power for acceleration, fuel economy, and charge acceptance during energy recovery from regenerative braking. Because the battery pack cost, durability, and life also affect the cost and reliability of the vehicle, any parameter that affects the battery pack must be optimized.

Battery module temperature uniformity is one such parameter. Depending on the electrochemical couple used in the battery, the optimum operating range is different. Some systems such as lead-acid, NiCd, Li ion, and NiMH batteries operate reasonably well near room temperature. Other systems, such as Li polymers, may need to operate at elevated temperatures, and systems such as NaS require operating temperatures around 330$^{o}$C. These high-temperature systems need active thermal management systems. Battery systems that operate at ambient temperatures can also benefit from battery thermal management systems. Generally, higher temperatures improve the battery's performance because of increased electrochemical reaction rates; however, the battery's lifetime decreases because elevated temperatures increase corrosion. If temperature uniformity can be obtained within and between modules, then, the pack can operate closer to its desired optimum operating temperature range.

Another important impact of a battery pack’s operating temperature is the electrical balance among modules in the pack. The performance of a battery pack depends on the performance of individual modules. If the cells and modules in the pack are at different temperatures, each module will be charged/discharged slightly differently during each cycle. After several cycles, modules in the pack will become unbalanced, degrading the pack’s performance.

HEV charging/discharge profiles are generally more aggressive than those of EVs, which results in greater heat generation. EV batteries are high specific energy; HEV batteries are high specific power. Thermal issues in an HEV pack, then, are of more concern than thermal issues in an EV pack and thus, a thermal management system is required for HEVs.

To optimize the performance of a battery pack, the thermal management system should deliver (1) optimum operating temperature range for all modules, (2) small temperature variations within a module, and (3) small temperature variations among various modules. However, the thermal management system must be compact and lightweight, easily packaged in the vehicle, reliable, and low-cost. It must also allow easy module access for service and use minimum power for fans and pumps.

In this paper we provide an overview of heat generation in battery modules and of related work on batteries and EV packs. We then discuss the results of a thermal analysis in battery modules and packs, and thermal imaging techniques that can assist in evaluating the thermal behavior of modules and packs.

## Background

### *Heat Generation*

Heat is generated in a battery cell by (1) entropy change from electrochemical reactions and (2) Joule's effect (or ohmic heating) caused by current transfer across internal resistances and overpotential. For some electrochemical pairs, another electrical energy loss (and thus heat generation) could result from overcharging a fully charged cell.

The heat generation rate in a cell can be calculated from Eq. 1 [1-3]:

$$q = - I [T (dE/dT)] + I(E-V) \quad (1)$$

where:

q = heat generation rate (W)
I = current (A); I > 0 for discharge and I < 0 for charge
T = temperature (K)
dE/dT = temperature coefficient (V/K)
E = equilibrium cell voltage or open-circuit potential (V)
V = cell voltage or cell potential (V).

The first term in Eq. 1, -I [T (dE/dT)] is heat generated or consumed because of the reversible entropy change resulting from cell electrochemical reactions. The second term I(E-V) is heat generation resulting from ohmic and other irreversible effects present in the cell. At practical EV and HEV rates, the first term is usually small compared to the second term. Thus, the heat is generated and released from the cell during both charge and discharge[2]. If the heat generated in the cell/module is not removed, it is stored, raising the temperature of the cell/module.

A battery pack comprising many modules will follow the thermal behavior of individual modules. In addition, interconnecting cables could add heat to the modules. To control the temperature of a battery pack in its optimum temperature range, heat may need to be rejected from modules during hot weather and added during cold weather. Battery pack thermal management and control could be achieved by air or liquid systems, insulation, thermal storage (phase-change material), active or passive approaches, or a combination.

### *Review of Related Work*

In this section, we review some of the work reported in the open literature to support statements made in the introduction and provide a basis for this work. Anderson compiled studies conducted between 1984-1988 for starting, lighting, and ignition (SLI) batteries in more than 5 million vehicles[4]. He reported that the life cycle of SLI lead-acid batteries decreases linearly with increasing temperature while the charge efficiency increases linearly (5% at -29°C to 35% at 82°C). Nelson and coworkers studied thermal control of electric vehicle batteries comparing seven different electrochemical pairs[5]. They concluded that even battery systems at near-ambient temperatures need thermal control.

Sharpe and Conell studied the effect of temperature on lead-acid battery charging and found that the charge acceptance rates dropped as the temperature dropped, especially below 0°C[6]. Dickinson and Swan evaluated the performance and life of several lead-acid EV battery packs[7], finding that the temperature gradient between modules reduces overall pack capacity. They recommended maintaining an even temperature distribution in the pack and a temperature of 35°C to 40°C for existing lead-acid batteries. Wicks and Doane investigated temperature-dependent performance of a lead-acid EV battery[8]. They found that the efficiency and maximum operating power increase with temperature over a range of -26°C to 65°C.

Burch and co-authors developed an enclosure using variable conductance vacuum insulation for high-temperature batteries such as sodium-sulfur[9]. McKinney describes thermal management of lead-acid batteries for an EV with electrolyte circulation pumps cycled and cooled by both forced air and natural convection[2]. Barnes and coworkers employed a phase-change material for cooling and temperature control of lead-acid modules[10].

Lee outlined a methodology for battery thermal modeling[11]. He proposed a thermal model based on three equations: (1) a typical differential equation energy balance, (2) a heat generation equation, and (3) the boundary condition equation that was based on linear heat transfer in the boundary region of the model (the case and electrolyte). Solving the three equations simultaneously yields temperature distribution in the core with time.

Newman and Tiedemann presented equations for a block-shaped three-dimensional battery module with uniform heat generation throughout[12]. The model assumed a constant battery wall temperature at all the outside surfaces at all times. Chen and Evans studied heat effects in batteries using two-dimensional transient conduction analysis of the battery stack with convective heat transfer at the battery boundaries[1]. Pals and Newman investigated thermal effects in a battery module from an overall energy balance perspective[3].

Our approach in obtaining thermal behavior of modules is similar to the cited work; however, we use a state-of-the-art finite element analysis software and extend the analysis to HEV packs. We also support the analytical work with experimental thermal imaging.

### *Battery Thermal Management System in Market-Ready EVs*

Most market-ready EVs have some kind of battery thermal management system. The following vehicles use air as the medium for battery pack cooling and heating: the General Motors EV1, the Chevrolet S-10 electric pickup, the Ford Ranger EV, and the Chrysler EPIC minivan (all with sealed lead-acid battery packs); the Toyota RAV4 electric with a nickel metal hydride battery pack; and the Nissan Prairie Joy with lithium ion battery modules. In the Honda EV Plus, circulating an organic fluid in jackets surrounding each module controls the temperature of its nickel metal hydride battery pack.

## Approach and Results

Our approach to obtaining thermal performance — that is, temperature distribution — in modules and packs is described below. First, using a finite element analysis software, the two-dimensional or three-dimensional transient or steady state heat conduction equation is solved for a set of modules at the beginning of the pack. If we are only interested in an average battery temperature, we ignore conduction and assume a single temperature for the modules. In selecting this set of modules, we take advantage of symmetry to solve for the minimum number of modules or even sections of a module to reduce computational efforts. Using an iterative process, we use the energy balance between the module surface temperature and its surroundings to find the overall temperature change in the fluid. Temperature distribution in any module in the pack could be obtained by using the superposition principle and overall energy balance.

Based on this approach, we evaluated the thermal performance of modules and packs from Ford, General Motors, and their suppliers. Because specific designs are proprietary, we will present for illustrative purposes typical results for a hypothetical, but realistic, module and pack. This example shows how the approach and tools we used can yield information on the module and pack behaviors and insight on design changes.

### *Module and Pack*

For our analysis, we used a rectangular, valve-regulated, lead-acid battery module (Figure 1) with the following characteristics:

- Number of cells: 6
- Nominal voltage: 12 V
- Capacity: 20 Ah
- Overall dimensions: 0.11 m width, 0.16 m length, and 0.15 m height
- Plastic case thickness: 0.002 m
- Weight: 8 kg
- Heat generation rate: 5.83 W/cell or 35 W/module
- Cell core average thermal conductivity: 6 W/mK
- Plastic case (polypropolyne) thermal conductivity: 0.25 W/mK
- Overall module heat capacity: 900 J/kgK.

We selected air at 25°C for cooling the module and a heat transfer coefficient of 35 $W/m^2$ K on all side battery surfaces. This coefficient is equivalent to a modest forced convection value with air. For simplicity we assumed that heat generation is uniform throughout the module core and constant with time (no heat in the plastic case). The module core material was assumed to be of a single homogeneous material although it may consist of layers of lead grid, positive and negative pastes, a separator saturated with acid, and connectors. The thermal properties of the core region of the module were estimated from individual literature values based on weight averaging and using parallel/series thermal resistances. The cell interconnects were not modeled. With these assumptions, a two-dimensional analysis was acceptable and thus performed.

Figure 2 shows the temperature distribution in a horizontal cross-section of this module at *steady state.* The observations from the results of this example are applicable to real batteries. The solution is symmetrical with the maximum temperature of 45.4°C at the center of the module, and coolest points are at each corner because of heat loss at both sides. There is approximately a 4.5°C difference between the maximum and minimum temperature in the core part of the module, and approximately a 3-4°C difference across the thin polypropylene case, indicating that the thin

plastic case imposes a large resistance to heat transfer in the module. If the case had a thermal conductivity equivalent to that of the cell core, the maximum module temperature would have dropped to about 41.7°C, but the core temperature difference would have remained around 4.5°C. Another large resistance between the cooling air at 25°C and the surface of the battery at 35-38°C is due to a relatively low heat-transfer coefficient in air. If the heat transfer coefficient is increased to 100 W/m$^2$ K, the maximum module temperature would have dropped to 36.7°C with a 4.5°C temperature difference still in the core, but this requires much higher air flow rates.

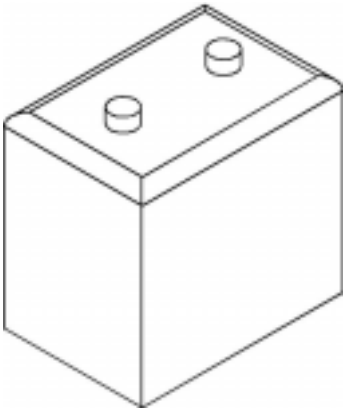

**Figure 1. Schematic of the Analyzed Module**

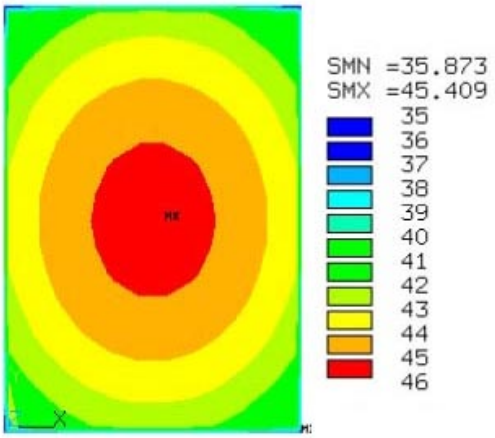


**Figure 2. Steady-State 2-D Temperature Distribution in the Module**

The hypothetical battery pack we considered as a high-power energy source for an HEV application consisted of 30 modules in 10 rows and 3 columns (Figure 3). We selected 0.08 kg/s of air to be used for cooling the pack entering from one end and exiting at the other end. The pack was assumed to be insulated from the top, the bottom, and on the sides. We assumed one-third of the flow rate is going through each column and that air is circulated equally around each module. The air gap was selected so that the air-side heat transfer coefficient was estimated to be 35 W/m$^2$ K. Using the same properties used for a single module, we used finite element analysis to obtain the temperature distribution in the pack. Figure 4 shows the variation of air temperature, module surface temperature, and module centerline temperature along the length of the path in the flow direction at steady state. Figure 5 shows the temperature distribution in the pack at steady state.

The air temperature rises by 1.3°C as it passes by each module. This, in turn, causes the average battery temperature to increase by 1.3°C in the direction of the flow, resulting in a variation of 13°C between the first and last battery. There is also a variation of about 4.5°C within each module. Although this cooling arrangement is not ideal, it is much better than placing the pack in a closed box (Figure 6) with some heat loss around it. Although the above analysis was for steady state, which may require a 2-3 hour continuous driving cycle, our analysis indicates that transient cases exhibit similar trends.

We used this type of analysis to evaluate the impact of a design change for a proposed Optima Batteries module consisting of a number of spiral-wound valve-regulated lead-acid cells. Figure 7 shows the geometry of a two-dimensional section of the studied module with the purple area as cells, the red area as plastic casing, and the blue area as cooling air. Under certain design conditions, the maximum temperature was 52.3°C with temperature distributions in the module shown in Figure 8. Under the same conditions, adding holes in the middle of the plastic casing

(Figure 9) resulted in the maximum temperature to drop below 44.1°C with some reduction in temperature gradient in the modules (see Figure 10). Based on this analysis, the new Optima modules for high-power HEV applications now have holes between the inner cells.

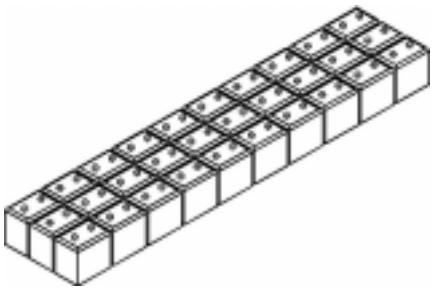

**Figure 3. Schematic of the Analyzed Battery Pack**

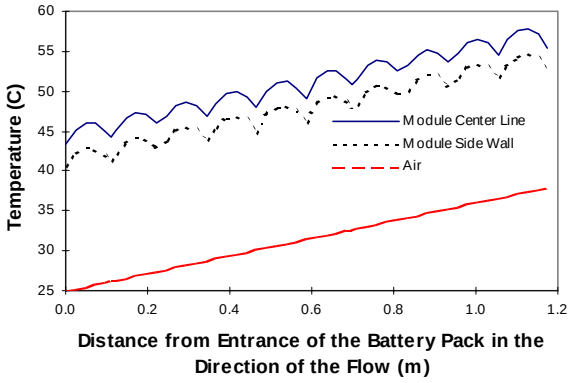


**Figure 4. Steady-State Air, Battery Surface, and Battery Center-Line Temperature in the Battery Pack**

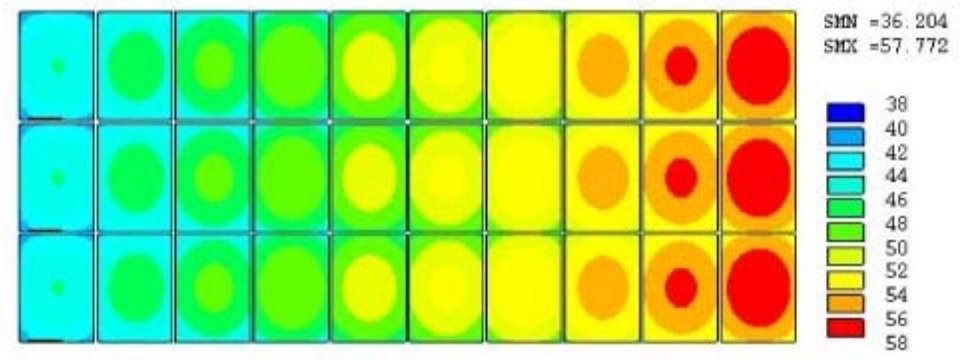


**Figure 5. Steady-State 2-D Temperature Distribution in Battery Pack with Air Flow Rate**

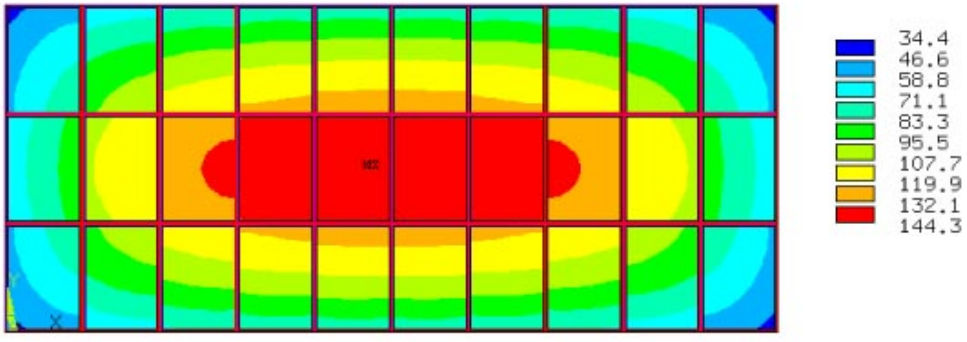


**Figure 6. Steady-State 2-D Temperature Distribution in an Enclosed Battery Pack**

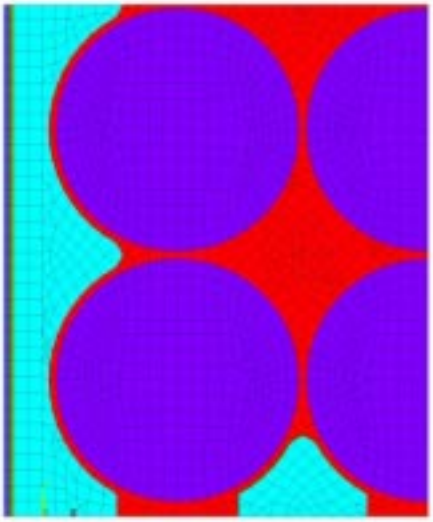

**Figure 7. Cross Section of a Proposed HEV Module** (purple areas are cells, the red area is plastic casing, and the blue area is cooling air)

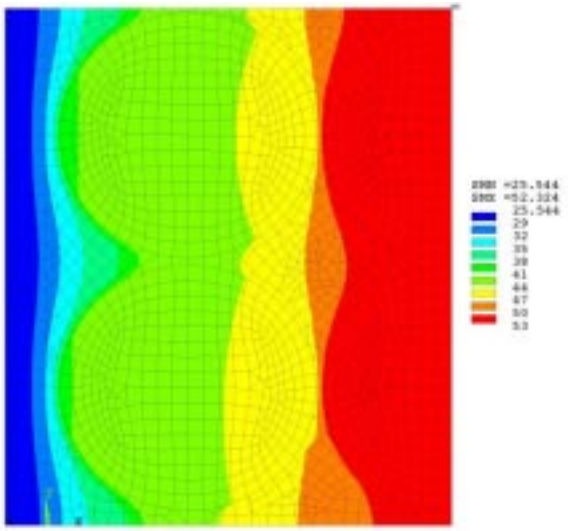

**Figure 8. Steady-State Temperature Distribution in the HEV Module with No Holes**

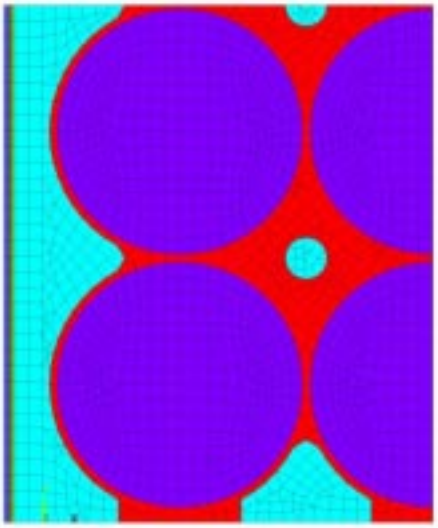

**Figure 9. Cross Section of the Proposed Module with Holes** (purple areas are cells, red area is plastic casing, and the blue area is cooling air)

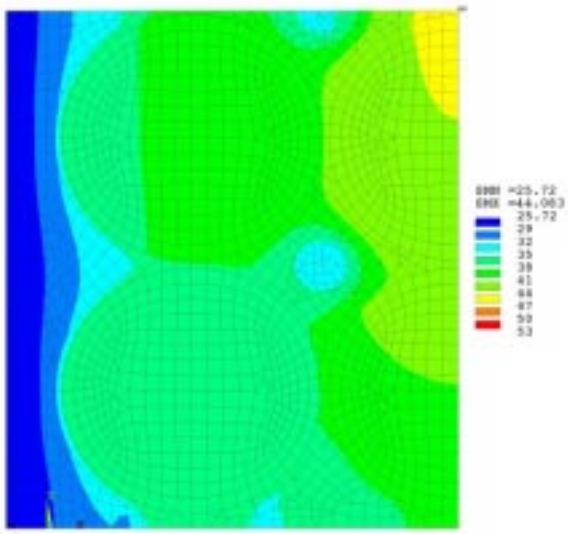

**Figure 10. Steady-State Temperature HEV Distribution in the HEV Module with Holes**

### *Thermal Imaging*

Obtaining thermal images of a battery module or a pack is a useful way to obtain information on temperature variation and compare that with analytical results. It is more productive and less intrusive than installing many temperature sensors on the walls. We used two techniques to obtain thermal images from modules: infrared (IR) photography and liquid crystal (LC) thermography.

IR imaging uses a special camera to capture IR radiation from an object. This thermal radiation is converted to surface temperature readings on all the points of the object. With an IR camera/video, we can obtain real-time or still thermal images from any object with a resolution

of 0.2°C and vivid and dramatic colors. We obtained thermal images of several modules and a full view of the entire pack using an IR camera. Figure 11 shows the IR thermal image of an HEV module right after a very high current peak passing through the module during a typical HEV charge/discharge cycle. The temperature scale is at the bottom of the figure. The thermal image indicates that under the high current profiles, the temperature at the top of the battery is higher than in the lower portion of the cell. This is because the heat generation is higher in the lead cell interconnects than in the cells. The hot spots at interconnects creates a vertical temperature gradient in the cells/module. The next generation of this type of HEV modules uses lower resistance cell interconnects to reduce hot spots and vertical gradients as we found in our later thermal imaging studies.

The IR technique is excellent for obtaining real-time, thermal images from a non-enclosed battery module or pack. However, if the pack enclosure is made of non-IR transmittable materials such as metals, glass, and almost all clear plastics, this technique is not optimal for obtaining thermal images.

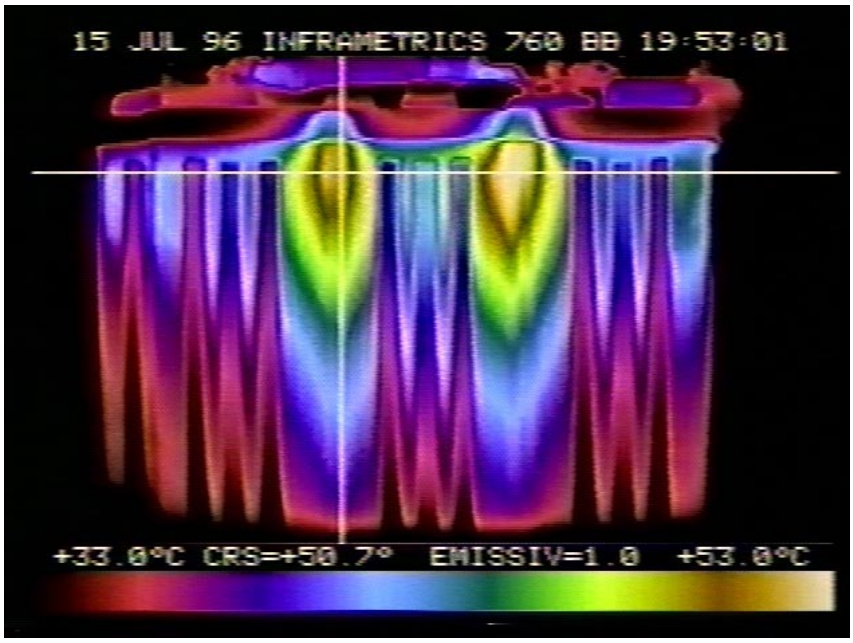


**Figure 11. An Infrared Thermal Image of an HEV Battery Module Immediately after a Large Current Peak during a Typical HEV Cycling**

In the LC thermography technique, liquid crystals with appropriate color/temperature range are applied to an object's surface. A liquid crystal changes color depending on its temperature. By applying a very thin layer, the object's thermal performance does not change, but as the object's temperature changes, so does the color of the liquid crystal layer. If the color-temperature relation is calibrated, we can easily determine the temperature variation from the color changes. With either video or still photography, we can capture thermal images from the liquid crystals with resolution of around 1°C. With special optical equipment, the resolution can be around 0.4°C. We used this technique for determining the thermal behavior of a simulated HEV pack. The technique gave us information on how to improve the pack from a thermal management perspective. Although LC thermography is not as accurate and flexible as the IR thermography, the color changes can be seen through any transparent enclosure. This technique is particularly useful for capturing thermal images of a battery pack in a clear enclosure with ventilation air through the pack.

The advantage of IR thermography is a wider temperature range, higher accuracy, and more vivid colors. The advantage of LC thermography is that it does not need special equipment and is visible through optically transmittable materials.

## Conclusions

The battery pack performance, and thus the performance of an EV or HEV, is affected by its operating temperature and the degree of temperature gradient in the pack. Thermal issues are of more concern in an HEV pack because of higher power and more aggressive charge/discharge profile. Thermal analysis must be performed to properly design thermal management systems for EVs and particularly HEVs. We used fundamental heat transfer principles and finite element analysis software to predict the thermal performance of HEV modules and packs. We obtained temperature distributions in a hypothetical module and pack. Even with reasonable air flow rates, the temperature in the pack can vary significantly. A pack with no air flow can reach unacceptably high temperature levels. Attention must be given to proper thermal design of the modules and packs. Our analysis indicated that adding ventilation holes improved the thermal performance of an HEV battery module. IR and LC thermography were used to obtain thermal images of an HEV module and a simulated HEV pack. These techniques are useful for assessing thermal behavior and could be used to point to trouble areas and provide insight to improved designs.

## Acknowledgments

The U.S. Department of Energy Office of Advanced Transportation Technologies funded this work as part of the cost-shared HEV program with General Motors, Ford, and Chrysler. Cycling of HEV modules for obtaining IR thermal images was conducted at AeroVironment, Inc., of Monrovia, CA. Keith Wipke and Tom Thoensen of NREL assisted with liquid crystal thermography.

## References

1. Y. Chen and J. Evans. *Journal of Electrochemical Society*, 1994, Volume 141, pp. 2947-2952.

2. B. McKinney, G. Wierschem, and E. Nrotek. "Thermal Management of Lead-Acid Batteries for Electric Vehicles," presented at the Batteries for Electric Vehicle-Research Development and Testing Conference, Detroit, MI, February 28, 1993.

3. C. Pals and J. Newman. *Journal of Electrochemical Society*, 1995, Volume 142, pp. 3274-3279.

4. R. Anderson. "Requirements for Improved Battery Design and Performance," *SAE Transactions*, September 6, 1990, Volume 99, pp. 1190-1197.

5. P. Nelson, V. Battaglia, and G. Henriksen. "Thermal Control of Electric Vehicle Batteries," *Proceedings of the 30th Intersociety Energy Conversion Engineering Conference*, July 30-August 4, 1995, Volume 3, pp. 267-273.

6. T. Sharpe and R. Conell. "Low-Temperature Charging Behavior of Lead-Acid Cells," *Journal of Applied Electrochemistry*, 1987, Volume 17, pp. 789-799.

7. B. Dickinson and D. Swan. "EV Battery Pack Life: Pack Degradation and Solutions," *Proceedings of the Future Transportation Technology Conference and Exposition*, 1995, pp. 145-154.

8. F. Wicks and E. Doane. "Temperature Dependent Performance of a Lead Acid Electric Vehicle Battery," *Proceedings of the 28th Intersociety Energy Conversion Engineering Conference*, 1993.

9. S. Burch, R. Parish, and M. Keyser. "Thermal Management of Batteries Using a Variable-Conductance Insulation (VCI) Enclosure," Golden, CO: National Renewable Energy Laboratory, NREL/TP-473-7783, May 1995.

10. S. Barnes, F. Fleming, W. Longardner, and A. Rafalovich. "Thermal Management for HEV Valve-Regulated Lead-Acid Batteries," *Proceedings of the 12th Annual International Electric Vehicle Symposium*, December 1994, pp. 27-37.

11. J. Lee. "Battery Thermal Modeling - The Methodology and Applications," *Proceedings of the Symposium on Electrochemical and Thermal Modeling of Batteries, Fuel Cells and Energy Conversion Systems*, 1986, Volume 86-12, pp. 206-215.

12. J. Newman and W. Tiedemann. "Temperature Rise in a Battery Module with Constant Heat Generation," *Journal of Electrochemical Society*, April 1995, Volume 142, pp. 1054-1057.

## Appendix A. Heat Transfer Analysis of Modules and Packs

Below we present the fundamental heat transfer equations we used for analyzing thermal performance of modules and packs. As we discussed in the body of the paper, as heat is generated in a module, it is either removed/rejected to the surrounding area, accumulated in the module, or both. It is also possible that if the surrounding area is at a higher temperature than the module, heat will be transferred into it. An overall energy balance on a battery module leads to:

$$q - h_b A_{bs} (T_{bs} - T_f) - \sigma \varepsilon F_{bf} A_{bs} (T_{bs}^4 - T_f^4) = M_b C_b (dT_{ba}/dt) \quad \text{(A-1)}$$

where

$q$ = heat generation rate in the module that could be a function of time (W),
$h_b$= heat transfer coefficient between battery surface and its surrounding fluid (W/m$^2$ K),
$A_b$ = battery surface area exposed to the surrounding fluid (m$^2$),
$T_{bs}$ = battery surface temperature (K),
$T_f$ = surrounding fluid temperature (K),
$\sigma$ = Stefan-Boltzman constant,
$\varepsilon$ = battery surface emissivity,
$F_{bf}$ = shape factor between the battery and its surroundings,
$M_b$ = module mass (kg),
$C_b$ = weighted-average module heat capacity (J/kg K),
$T_{ba}$ = average module temperature (K), and
$t$ = time (s).

The second term in Eq. A-1 is the convective heat transfer between the battery surface and its surrounding fluid. The third term is the radiative heat transfer from the battery surface to its surroundings. The radiative term is usually small compared to the convective term if temperatures are below 100°C, so it is ignored for lead-acid and other near ambient batteries.

In Eq. A-1, we used an average battery temperature. However, in reality, a three-dimensional temperature distribution exists in the modules. The three-dimensional heat conduction equation for the module should be solved to obtain temperature distribution. In Cartesian coordinates, the heat conduction equation for an element of the module can be expressed as

$$\rho C_p \partial T/\partial t = k_x \partial^2 T/\partial x^2 + k_y \partial^2 T/\partial y^2 + k_z \partial^2 T/\partial z^2 + Q, \quad \text{(A-2)}$$

where $\rho$ is local density (kg/m$^3$); $C_p$ is local specific heat (J/kg K); $k_x$ , $k_y$ , and $k_z$ are local thermal conductivities (W/m K) in different directions; and Q is the local heat generation rate per unit volume (W/m$^3$ ), which could vary with time and location. Eq. A-2 could be solved knowing the boundary conditions and initial conditions for the module. For cylindrical batteries, the conduction equation is expressed in cylindrical coordinates. The boundary condition around the module depends on the type of cooling/heating provided; it could be insulated, convectively cooled/heated with a fluid, or conductivity cooled/heated with phase-change materials or indirect contact with a liquid.

Eq. A-2 could be solved analytically only for very simple geometries and simple boundary

conditions. Under some circumstances and with simplifying assumptions, Eq. A-2 could be simplified into two- or one-dimensional cases and then solved analytically. For more realistic battery shapes and boundary conditions, Eq. A-2 needs to be solved with numerical techniques. We used a commercial finite element analysis software to solve for temperature distribution in HEV modules. After solving for temperature distribution in a module and obtaining surface temperatures, we obtain the temperature distribution in the pack. If the pack configuration or boundary conditions are not simple, numerical techniques and computer-aided engineering tools can be used. If complex fluid flow exists, computational fluid dynamics codes can also be used.

We use the overall energy balance to obtain the temperature distribution in a pack of modules. For example, if a certain amount of a fluid is passed around a module, the fluid temperature change can be obtained from overall energy balance for the module:

$$h_b A_{bs} (T_{bs} - T_f) = [m_f C_f (T_{out} - T_{in})]_{module} . \quad (A\text{-}3)$$

Note that $T_f$ is average fluid temperature, $m_f$ is the mass flow rate of fluid around each module, $C_f$ is the fluid specific heat, $T_{in}$ is the incoming fluid temperature to the module, and $T_{out}$ is the temperature of the fluid leaving the module. The fluid can pass around the modules in series, in parallel, or in a combination. If the modules are in series and the same fluid is going over each module, the total temperature rise in the fluid depends on the summation of all the heat added to the fluid. The overall temperature change in the fluid can be obtained from the overall energy balance

$$N [q - M_b C_b (dT_{ba} /dt)] = [m_f C_f (T_{out} - T_{in}) - M_f C_f (dT_f/dt) ]_{pack}. \quad (A\text{-}4)$$

where N is the number of modules in the path of $m_f$ (fluid flow rate) and $M_f$ is mass of the fluid. The second terms on each side of the equation are thermal inertia of the module and the fluid, respectively, and could be ignored for short-term transient and steady state cases.

We used the above equations and approach to analyze the thermal behavior of the battery modules and pack as described at the beginning of Approach and Results section.